2

CONF-9210276--2

LBL-32955
UC-404

Lawrence Berkeley Laboratory
UNIVERSITY OF CALIFORNIA

Materials Sciences Division

Presented at the Fourth NEC Symposium on Fundamental Approaches in New Material Phases, Tokyo, Japan, October 11–15, 1992, and to be published in the Proceedings

Theory of Normal and Superconducting Properties of Fullerene-Based Solids

M.L. Cohen

October 1992

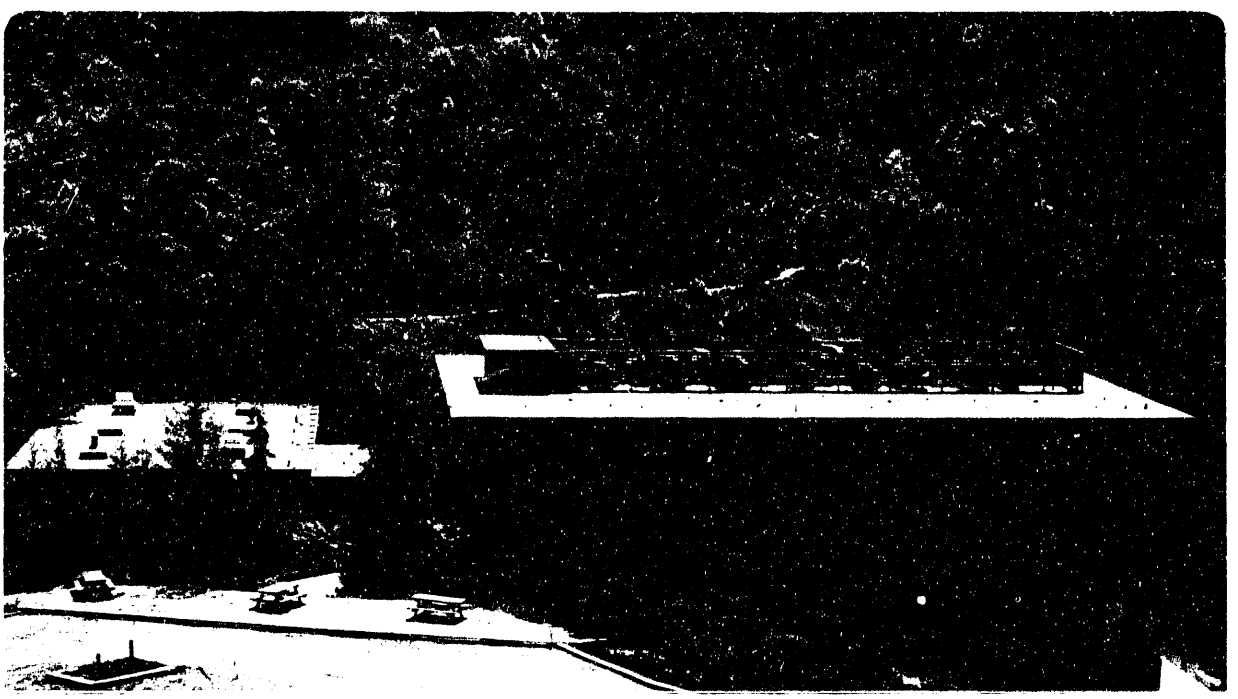

Prepared for the U.S. Department of Energy under Contract Number DE-AC03-76SF00098

LBL--32955

DE93 007722

Theory of Normal and Superconducting Properties of Fullerene-Based Solids

Marvin L. Cohen

Department of Physics
University of California

and

Materials Sciences Division
Lawrence Berkeley Laboratory
University of California
Berkeley, California 94720

October 1992

This work was supported by NSF Grant No. DMR91-20269 and by the Director, Office of Energy Research, Office of Basic Energy Sciences, Materials Sciences Division, of the U.S. Department of Energy under Contract No. DE-AC03-76SF00098.

LBL-32955
UC404

THEORY OF NORMAL AND SUPERCONDUCTING PROPERTIES OF FULLERENE-BASED SOLIDS

Marvin L. Cohen

Department of Physics, University of California at Berkeley, and
Materials Sciences Division, Lawrence Berkeley Laboratory,
Berkeley, CA 94720, U.S.A.

Abstract

Recent experiments on the normal-state and superconducting properties of fullerene-based solids are used to constrain the proposal theories of the electronic nature of these materials. In general, models of superconductivity based on electron pairing induced by phonons are consistent with electronic band theory and analyses of the measured normal-state transport properties. The latter experiments also yield estimates of the parameters characterizing these type II superconductors. It is argued that, at this point, a "standard model" of phonons interacting with itinerant electrons may be a good first approximation for explaining the properties of the metallic fullerenes.

Introduction

The high level of interest and activity since the discovery of C_{60} [1] in the area of fullerene-based solids has yielded "answers" and "new puzzles" related to the properties of these fascinating materials. Here we attempt to focus more on what appears to be a body of knowledge representing the "answers" to reasonable well-defined questions about the fullerenes with the goal of giving at least a temporary but reasonably complete description of a subclass of these solids. Of course, the experimental measurements are still open to interpretation, and here only one view is presented. The goal is to present a "standard model" which is supported by a number of experimentalists and theorists and to use this model as a basis for interpretation. Eventually, perhaps the "new puzzles" will shatter the standard model, but it is also reasonable to expect that these puzzles may be explainable with only modifications of the model.

Since the C_{60}-based solids are the most studied, the focus here will be on the electronic and superconducting properties of these materials. Perhaps future studies of solids based on C_{70} or other molecules in this family C_{20+2h} with 12 five-fold and h six-fold rings will be of equal interest or yield even more valuable information.

This paper begins with a description of the standard model for electronic structure and superconductivity. Some discussion of the evidence for this interpretation is presented followed by a few examples of alternative views and conflicting experiments.

The Standard Model

It is natural to begin a study of a new material or class of materials with tools that have been tested with success for so-called conventional materials. The covalent nature of the C_{60} molecular bonds and their similarity to graphite suggest that models used for explaining graphite and intercalated graphite may be sufficiently robust to explain properties of fullerenes. The interlayer bonding in graphite has van der Waal's character which is also present in fcc C_{60} between molecules. The fact that the molecules themselves contain a finite number of atoms does cause concern particularly

for excited states where electrons and holes are confined to a molecule. For example, studies of confinement of excitons in semiconductor clusters such as ZnSe have revealed unusual behavior. However, in the standard model discussed here, expected effects of this kind and other correlation effects will be ignored. These omissions leave us with a one-electron type model for fcc C_{60} and for M_3C_{60} where M is an alkali atom.

Using the one-electron model as a basis for energy band structure calculations [2] has yielded consistent pictures of the electronic structure for fcc C_{60} and M_3C_{60}. The bonding characteristics, the relation of the energy levels in the solid to those of the molecule, and the doping from the M atoms are all consistent and reasonable when the interpretation of the experimental data is made within this one-electron "standard model."

The measured phonon spectrum and related experimental data also appear to be consistent with the above picture of the electronic properties. Hence, phonon experiments provide few if any direct challenges to the standard model and, in general, the phonons of the C_{60}-based solids are viewed as conventional. A nonstandard feature of the phonon spectrum is the wide range of frequencies arising because of the low energy intermolecular and high energy intramolecular vibrations. The former are also grouped into librational, vibrational, and alkali-atom based modes. Rotational motions of the C_{60} molecules in the undoped solid add to the zoo of possible lattice excitations. A list of phonon frequencies and their related symmetries is given in Table 1. Although the range and variety are large compared to those normally studied regular "one" by condensed matter physicists, the neutron [3] and Raman [4] data appear to yield a more or less standard view of the librational and vibrational modes.

Combining the phonons and electrons, we present a model of M_3C_{60} with an itinerant electron sea interacting with the phonons listed in Table 1. If standard electron-phonon theory is assumed, these interactions should give rise to electrical resistance and superconductivity through BCS [5] pairing. Although this description resembles a theorist's prediction of what a system of soccer ball molecules should do,

the model is post hoc and was introduced by many researchers to explain experimental measurements. In fact, up to now, little has been predicted by theorists in this area; mostly, they have followed the lead of the experimentalists and provided explanations for the observations.

Transport Properties and Superconductivity

One test of the standard model for the metallic fullerenes is an analysis of their transport properties. In particular, K_3C_{60} has been viewed as an ionic metal with charge transferred from the K atoms to the molecules and interstitial region. From a band structure point of view, when alkali atoms occupy the two interstitial tetrahedral sites and the octahedral site in fcc C_{60} solid, the outermost s electron dopes the system yielding t_{1u} derived bands which are half full. This picture implies that K_3C_{60} is uniformly doped and that a rigid band model is appropriate for the doped material. This view of a doped crystal does stretch the usual definition since the K to C ratio of atoms albeit small is not comparable to what is usually encountered for doped semiconductors. However, band structure calculations for K_3C_{60} and fcc C_{60} do generally support this conceptional approximation.

Since the Fermi level E_F lies in a region of the density of states which is rapidly varying, it is expected that relatively small changes in the lattice constant caused by pressure or by substitution of different alkali atoms will cause the density of states at E_F, $N(E_F)$, to be a sensitive function of these changes. This sensitivity is also the origin of the lack of consensus on the value of $N(E_F)$ among various calculations. Values in the range of 10 to 30 states per eV per C_{60} are ecommonly quoted. The Fermi surface is relatively less sensitive to the placement of E_F, and it is generally pictured as having multiple electron-like and hole-like bands.

In the standard model, the temperature dependent resistivity should provide a measure of the electron-phonon scattering and, hence, the electron-phonon coupling constant λ_t where the subscript t indicates the fact that λ_t is derived from transport data. For isotropic more or less ideal systems [6], λ_t can be taken equal to the superconducting electron-phonon coupling parameters λ. Hence, for an assumed

Coulomb repulsion μ or its frequency renormalized value μ^* and a knowledge of the phonon spectrum, one can estimate the superconducting transition temperature T_c.

For example, if we introduce the standard electron-phonon spectral function $\alpha^2F(\omega)$

$$\lambda = 2 \int_0^{\omega_m} \alpha_2 F(\omega) \frac{d\omega}{\omega} \tag{1}$$

where ω and ω_m are the phonon frequencies and the maximum phonon frequencies respectively. The Ziman resistivity formula [7] for the temperature dependent resistivity is

$$\rho(T) = \frac{m\tau^{-1}}{ne^2} \text{ , where} \tag{2a}$$

$$\tau^{-1} = \frac{2\pi}{k_B T} \int_0^{\omega_m} \hbar\omega \, \alpha^2_t F(\omega) \left[\cosh\left(\frac{\hbar\omega}{k_B T}\right) - 1\right]^{-1} d\omega \tag{2b}$$

is an inverse time, n is the electron density, and the subscript t again refers to transport properties. The connection between Eqs. (1) and (2) is usually made in the high temperature approximation where $\frac{\hbar\omega}{k_B T} \gg 1$. Ignoring the difference between λ and λ_t, at high T the inverse relaxation time is

$$\tau^{-1} = \frac{2\pi}{\hbar} \lambda k T \ . \tag{3}$$

This illustrates the linear dependence on T of the resistivity at high T which is found in most solids. The slope of this curve yields a measure of λ.

For K_3C_{60}, the wide range of phonon frequencies makes an analysis of $\rho(T)$ particularly interesting. Because of the high frequency phonons, the linear portion of the $\rho(T)$ curve is only attained at very high T. Recent measurements [8,9] on single crystals from the superconducting transition temperature T_c up to 260 K are given in Fig. 1. A fit of Eq. (2) to these data reveals the importance of various phonon modes in the scattering. This analysis has implications for evaluating theoretical proposals of

phonon-induced electron pairing by assuming that the electron-phonon processes contributing to λ_t are similar or identical to those contributing to λ. The difference between $\lambda^2_tF(\omega)$ and $\alpha^2F(\omega)$ arises mainly through the wavevector dependence of the electron-phonon coupling. For K_3C_{60}, this effect is probably not large [6].

To obtain a rough idea of the magnitudes of the relevant parameters, one can use an Einstein phonon spectrum approximation to Eq. (2) with an average coupling λ_E and a phonon frequency ω_E; hence

$$\alpha^2_tF(\omega) = \frac{1}{2}\,\lambda_E\,\omega_E\,\delta\,(\omega - \omega_E) \quad . \tag{4}$$

Fitting this oversimplified model to the data yields $\lambda_E = 0.6$ and $\omega_E = 400$ K. Two conclusions from this model are that $\lambda \lesssim 1$ and that phonon frequencies above and below 400 K are needed to explain $\rho(T)$ and the superconducting T_c.

If we limit λ to a range < 1.5, then it is appropriate to use a McMillan [10] type equation for T_c

$$T_c = E_D\, e^{-\left(\frac{1}{\lambda^* - \mu^*}\right)} \tag{5}$$

where E_D is a constant of order unity times an average phonon frequency and $\lambda^* = \lambda/(1+\lambda)$. Because of the difficulty in calculating the Coulomb parameter μ, it is common practice to use standard estimates or to scale μ or μ^* directly. Almost all superconductors examined with BCS theory have μ^* values in the range of 0.1 to 0.3. The values of E_D or related averages of phonon frequencies and λ are the distinguishing features of the various phonon-induced pairing theories. Jishi and Dresselhaus (JD) [11] choose an average phonon frequency and λ, (E_D,λ) of about (500 K, 1) and emphasize the importance of lower frequency intramolecular modes. Schlüter *et al.* (SLNB) [12] choose values near (1000 K, 1) and focus on contributions from a broad range of H_g mode frequencies. Varmal *et al.* (VZR) [13] suggest that high frequency H_g modes are important and use values of the parameters near (2000 K, 0.5).

In principle, the $\rho(T)$ curves can be used to determine the role of the various phonon contributions to λ_t and, hence, evaluate the appropriateness of the various theoretical models. The fits of the three models discussed above to the $\rho(T)$ curve are given in Fig. 1. If the curves are fixed at the value of $\rho(T = 260\ K)$, then we find that the SLNB and VZR models do not yield as good a fit as the JD model. The fit is greatly improved by adding coupling to phonon modes below 200 K. In particular, when a mode at 150 K is added (Fig. 2), all three models give results consistent with experiment. It has been argued that low frequency electron-phonon couplings should be expected and that they can arise from intermolecular translational modes, librations, and polarizations of the C_{60} molecules by alkali atom vibrations. The general conclusion of this study is that the superconducting T_c is consistent with electron-phonon induced pairing via a broad range of intramolecular phonon frequencies. This analysis also yields a ratio of $2\Delta/k_BT_c \approx 3.6 - 4.0$ which is roughly consistent with infrared [14] and tunneling [15] measurements.

Another feature of the analysis of the normal state resistivity for $T > T_c$ is the determination of the dimensionality of the system through a study of the properties of the superconducting fluctuations. In conventional 3D superconductivity, paraconductivity arising from fluctuations is not observed unless considerable disorder is introduced to prove an effectively short coherence length. For K_3C_{60} and Rb_3C_{60}, the relatively short coherence lengths make a study of the paraconductivity advantageous even though it is expected that these systems are 3D in character. In fact, experiments reveal that this is the case and there is no low-dimensional cross-over.

In the cases studied, the resistively determined T_c's are 19.8 K and 30.2 K for K_3C_{60} and Rb_3C_{60} respectively, and the excess conductivity given by [16]

$$\sigma' \sim t^{-(4-d)/2} \qquad (6)$$

where $t = (T - T_c)/T_c$, allows a measurement [17] of the dimensionality d. For both cases, log-log plots of the data over almost two decades yield a slope of -1/2 and,

hence, imply d = 3. No effects of granular superconductivity are seen down to $t \sim 5 \times 10^{-4}$ suggesting a limit on the domain size of ~0.6 μm.

It is interesting to note that these are first observations of this kind for 3D superconductivity. They are made possible by the short coherence length and the relatively high resistivity of these C_{60}-based solids.

Some Superconducting Properties

In addition to the measurements of T_c, other measured properties of the superconducting state include the pressure dependence of the transition temperature $\partial T_c/\partial P$, the isotope effect parameters $\alpha = d\ \ell n\ T_c / d\ \ell n\ M$, and the temperature dependence of the upper critical field $H_{c2}(T)$.

A negative $\partial T_c/\partial P \sim -0.8$/Kbar for both K_3C_{60} and Rb_3C_{60} has been interpreted in terms of a decreasing $N(E_F)$ with decreasing lattice constant. This is consistent with the observation of increasing T_c with larger alkali atoms and, hence, larger lattice constants. This interpretation is based on the popular view that λ, which represents an averaged product of N(E) and the pairing potential V involves contributions dominated by intraball excitations for V and interball excitations for N(E) for E near E_F. Hence, the decreasing lattice constant results in a smaller bandwidth and $N(E_F)$ which, in turn, yields a lower T_c. A striking linear relation has been found [18] between the measured T_c and the calculated $N(E_F)$. This is not inconsistent with BCS behavior of T_c on λ for some ranges of λ.

The isotope parameter can be expressed in terms of λ^* and μ^* for moderate values of λ as

$$\alpha = \frac{1}{2}\left[1 - \left(\frac{\lambda^*}{\lambda^* - \mu^*}\right)^2\right] . \qquad (7)$$

This expression has an upper limit of 1/2 and no lower limit. It is possible [19] to obtain $\alpha > 1/2$ if anharmonic phonon effects are include. For most conventional superconductors, $\alpha \lesssim 1/2$, but reduced values are found for transition metals and high

T_c oxides. For M_3C_{60}, several values of α have been reported [20-24]. These values depend on the percentage replacement of ^{13}C for ^{12}C.

Experimental values of 0.3 to 0.4 are consistent with the electron-phonon pairing theories discussed earlier. There are constraints which depend sensitively on the phonon frequencies assumed most important for the pairing. For example, if $\alpha = 0.37$ and $T_c = 29$ K, then for an average phonon frequency of 1000 K, $\lambda = 0.81$, and $\mu^* = 0.19$, whereas a phonon frequency of 200 K requires $\lambda = 2.5$ and $\mu^* = 0.31$. The observation of a finite α in the range of 1/4 to 1/2 adds support to the standard model for these systems. If the reported values of $\alpha > 1/2$ are intrinsic to homogeneous M_3C_{60} systems, then the electron-phonon mechanism is still strongly supported but the role anharmonic phonons needs to be determined.

Measurements of the upper critical field $H_{c2}(T)$ can give information about transport and superconducting and normal state parameters such as the coherence length ξ_0 and the scattering time τ. There are differences between the data for single crystal and thin film or polycrystalline samples. Here we consider the measurements made on single crystal samples of K_3C_{60}.

The normalized resistivity of K_3C_{60} as a function of applied field [25] is given in Fig. 3. The resulting $H_{c2}(T)$ curve is presented in Fig. 4. Since the single-crystal transitions near T_c are relatively sharp, a good determination of $H_{c2}(T)$ and the relevant parameters can be made using standard theory for type II superconductors. Similar data are obtained for Rb_3C_{60}[25]. The resulting parameters extracted from the data are given in Table 2. In Table 2, $\xi(0)$ is the zero temperature coherence length, ξ_0 is the clean limit coherence length, τ is the zero temperature scattering time and ℓ is the mean free path. A fairly consistent picture for these materials results and these data yield parameters which are consistent with the microscopic theories of the underlying pairing mechanism.

Some Challenges to the Standard Model

Some researchers feel that it is naive to consider the M_3C_{60} system using the same model of a solid as one would use for common metals and semiconductors. In particular it is felt that electron-electron scattering effects and correlation should be dominant.

In fact, at first glance, the experimental $\rho(T)$ curve reminds one of the classic T^2 behavior for ρ arising from electron-electron scattering. The raw data do fit a T^2 curve fairly well, but when thermal expansion effects are included, the fit is less impressive. In addition, one expects a T^2 behavior of this kind only at low T so that it is probably not prudent to associate the "T^2 like" feature of Fig. 1 with electron-electron scattering.

When one considers the length scales associated with M_3C_{60}, again effects of electron-electron correlation are expected. For example, in K_3C_{60}, both the diameters of the C_{60} molecules and the nearest neighbor distances are about 10 Å. When two electrons are both on a molecule, strong correlation effects are expected. In addition, the band calculations yield narrow band widths even for states with charge concentrated between the molecules, and narrow band widths implying strong correlations.

Recent photoemission and inverse photoemission spectra [26,27] question the standard band models. One interpretation [26] suggests that alkali doping does not lead to a rigid filling of the lowest unoccupied molecular orbital band but causes charge transfer. Another model [27] suggests that doped C_{60} is a highly correlated system similar to the high T_c cuprates.

Because of the above considerations, several researchers have questioned the use of a conventional μ^* in explaining the superconductivity of M_3C_{60}. It is argued that correlation effects and large $N(E_F)$ can yield large values of μ and μ^*. In principle this is possible, but for most cases screening effects cancel the large values of $N(E_F)$when the $N(E)$ V_c (where V_c is the appropriately screened Coulomb potential) function is averaged over the Fermi surface.

Correlation effects between electrons on the same C_{60} molecule have been considered [28-30] as a mechanism for causing superconductivity. The theory is based on a Hubbard Model, and it is claimed that the normally repulsive Coulomb interaction has the effect of pairing electrons. Within this electron-electron model, the isotope effect is explained through isotopic variation in the matrix element for hopping between carbon atoms.

Conclusions

At present, there are interesting alternative models to the standard model and the experimental data are not conclusive. A somewhat conservative but defensible view is to keep the standard picture to a first approximation and to continue testing it until failures force a new picture. In this model, electrons are more or less itinerant and scatter from intramolecular phonons. For the superconducting state, electrons pair primarily via intramolecular vibrations and behave generally according to the BCS description of superconductors.

The above standard model may be viewed as dull by some researchers. But if it is a correct view, it does unify a lot of concepts about solids and demonstrates that spectacular properties are possible within this model when the relevant parameters are allowed to vary over a wider range.

Acknowledgements

Much of the work presented here was done in collaboration with V. H. Crespi, A. Zettl, X.-D. Xiang and J. G. Hou. This work was supported by National Science Foundation Grant No. FD91-20269 and by the Director, Office of Energy Research, Office of Basic Energy Sciences, Materials Sciences Division of the U. S. Department of Energy under Contract No. DE-AC03-76SF00098.

Table 1. Experimental phonon frequencies for intraball modes in *undoped* C_{60} of the correct symmetry to mediate electron-phonon coupling.Upon doping, the energies shift by a few percent.

Mode	ω(K)
H_g (1)	393
H_g (2)	629
H_g (3)	1022
H_g (4)	1071
H_g (5)	1581
H_g (6)	1799
H_g (7)	2055
H_g (8)	2266
A_g (1)	715
A_g (2)	2114

Table 2. Macroscopic superconducting state and normal state parameters of Rb_3C_{60} and K_3C_{60} single crystals (Ref. 25).

Parameter	Rb_3C_{60} (unit)	K_3C_{60} (unit)
T_c	30.0 (K)	19.7 (K)
dH_{c2}/dT	-3.8 (Tesla/K)	-1.34 (Tesla/K)
$H_{c2}(0)$	76 (Tesla)	17.5 (Tesla)
$\xi(0)$	20 (Å)	45 (Å)
ξ_0	40 - 55 (Å)	95 ± 15 (Å)
τ	$5.3 \pm 2.0 \times 10^{-15}$ (sec.)	1.7 ± 0.5 (sec)
ℓ	9 ± 3	31

Figure Captions

Figure 1. Theoretical fits of electron-phonon scattering models for the experimental temperature dependent resistivity (circles). The models are discussed in the text and referred to as VZR(solid line), SLNB (dashed line), and JD (dotted line). The normalization factor $\rho_0 = \rho(T = 260\ K)$.

Figure 2. The curves are the same as in Fig. 1 with an additional phonon mode at 150 K.

Figure 3. Normalize resistivity of single crystal K_3C_{60} near T_c for varying applied magnetic field. ρ_0 is the room temperature value and the insert shows the zero field temperature dependence of the normalized resistivity.

Figure 4. Temperature dependence of the upper critical field H_{c2} for K_3C_{60}.

References

1. H. W. Kroto, J. R. Heath, S. C. O'Brien, R. F. Curl, and R. E. Smalley, *Nature, 318* (1985) 162.
2. S. Saito and A. Oshiyama, *Phys. Rev. Lett., 66* (1991) 2637.
3. K. Prassides, J. Tomkinson, C. Christides, M. J. Rosseinsky, D. W. Murphy, and R. C. Haddon, *Nature, 354* (1991) 462.
4. M. G. Mitch, S. J. Chase, and J. S. Lannin, *Phys. Rev. Lett., 68* (1992) 883.
5. J. Bardeen, L. N. Cooper, and J. R. Schrieffer, *Phys. Rev., 106* (1957) 162; *108* (1957) 1175.
6. V. H. Crespi and M. L. Cohen, *Solid State Comm., 81* (1992) 187.
7. G. Grimvall, *The Electron-Phonon Interaction in Metals,* North-Holland Publishing Company, 1991, p. 210.
8. X.-D. Xiang, J. G. Hou, G. Briceño, W. A. Vareka, R. Mostovsky, A. Zettl, V. H. Crespi, and M. L. Cohen, *Science, 256* (1992) 1190.
9. V. H. Crespi, J. G. Hou, X.-D. Xiang, M. L. Cohen, and A. Zettl, *Phys. Rev.* (in press).
10. W. L. McMillan, *Phys. Rev., 167* (1968) 331.
11. R. A. Jishi and M. S. Dresselhaus, *Phys. Rev., B 45* (1992) 2597.
12. M. Schlüter, M. Lannoo, M. Needels, and G. A. Baraff, *Phys. Rev. Lett., 68* (1992) 526.
13. C. M. Varma, J. Zaanen, and K. Raghavachari, *Science, 254* (1991) 989.
14. L. D. Rotter, Z. Schlesinger, J. P. McCauley Jr., N. Coustel, J. E. Fischer, and A. Smith III, *Nature, 355* (1992) 532.
15. Z. Zhang, C.-C. Chen, and C. Lieber, *Science, 254* (1991) 1619.
16. L. G. Aslamasov and A. I. Larkin, *Phys. Letters, 26A* (1968) 238.
17. X.-D. Xiang, J. G. Hou, V. H. Crespi, A. Zettl, and M. L. Cohen, to be published.
18. A. Oshiyama and S. Saito, *Solid State Comm, 82* (1991) 41.
19. V. H. Crespi and M. L. Cohen, *Phys. Rev. B, 44* (1991) 4712.

20. T. W. Ebbeson, J. S. Tsai, K. Tanigaki, J. Tabuchi, Y. Shimakawa, Y. Kubo, I. Hirosawa, and J. Mizuki, *Nature, 355* (1992) 620.

21. A. A. Zakhidov, K. Imaeda, D. M. Petty, K. Yakushi, H. Inokuchi, K. Kikuchi, I. Ikemoto, S. Suzuki, and Y. Achiba, *Phys. Lett., A164* (1992) 355.

22. A. P. Ramirez, A. R. Kortan, M. J. Rosseinsky, S. J. Duclos, A. M. Mujsee, R. C. Haddon, D. W. Murphy, A. V. Makhija, S. M. Zahurak, and K. B. Lyons, *Phys. Rev. Lett., 68* (1992) 1058.

23. C.-C. Chen and C. M. Lieber, *J. of APS, 144* (1992) 3141.

24. D. S. Bethune, W. Y. Lede, M. S. De Vries, J. R. Salem, W. C. Tang, H. J. Rosen, C. A. Brown, *Surf. Sci.*, in press.

25. J. G. Hou, V. H. Crespi, X.-D. Xiang, W. A. Bareka, G. Briceño, A. Zettl, and M. L. Cohen, to be published; and J. G. Hou, V. H. Crespi, X.-D. Xiang, A. Zettl, and M. L. Cohen, to be published.

26. T. Takahashi, S. Suzuki, T. Morikawa, H. Katayama-Yoshida, S. Hasegawa, H. Inokuchi, K. Seki, K. Kikuchi, S. Suzuki, K. Ikemoto, and Y. Achiba, *Phys. Rev. Lett, 68* (1992) 1232.

27. R. W. Lof, M. A. van Veenendaal, B. Koopmans, H. T. Jonkman, and G. A. Sawatzky, *Phys. Rev. Lett, 68* (1992) 3924.

28. S. R. White, S. Chakravarty, M. P. Gelfand, and S. A. Kivelson, *Phys. Rev. B, 45* (1992) 5062.

29. S. Chakravarty, M. P. Gelfand, and S. A. Kivelson, *Science, 254* (1991) 970.

30. S. Chakravarty and S. A. Kivelson, *Europhys. Lett., 16* (1991) 751.

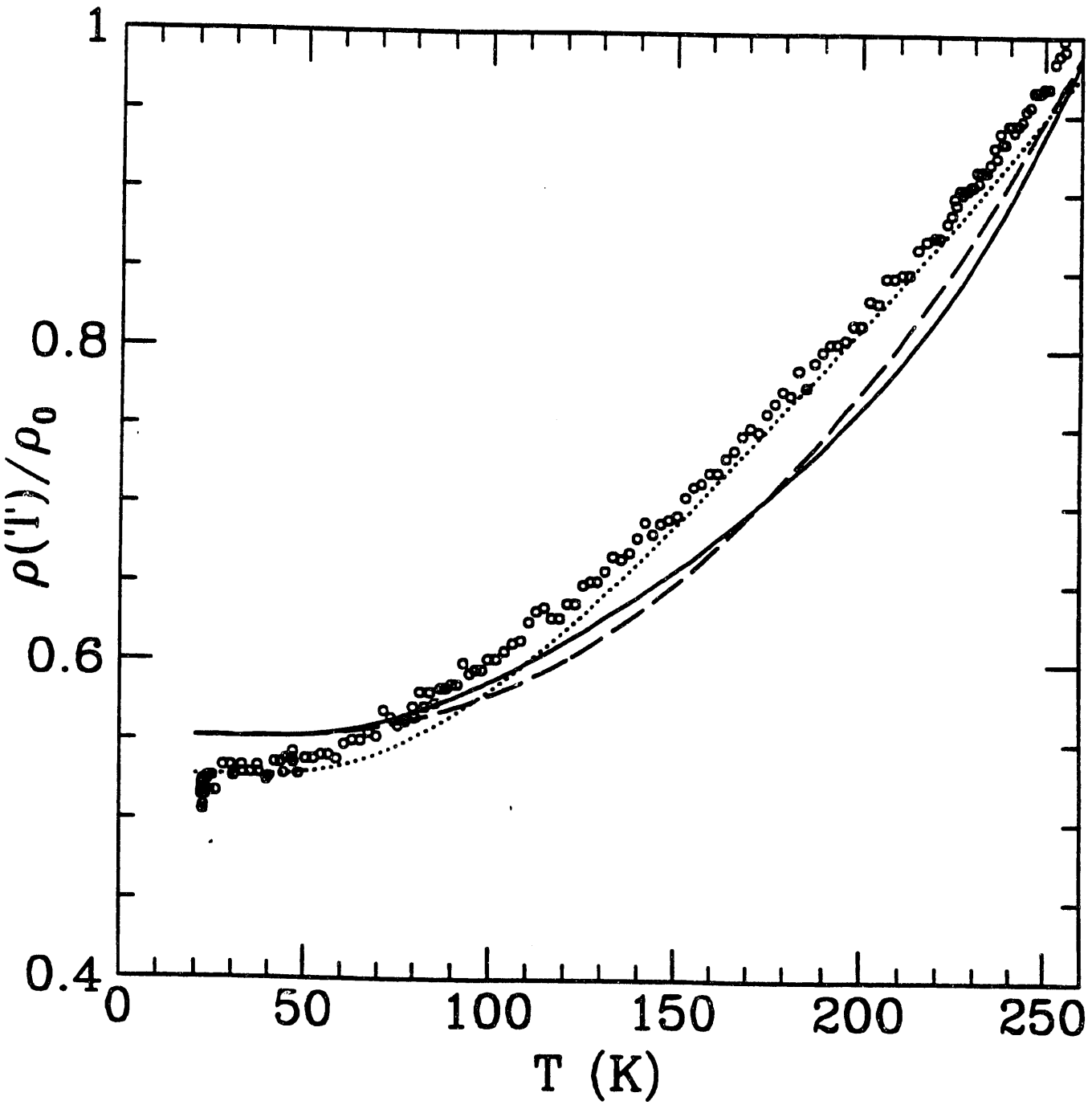

FIG. 1

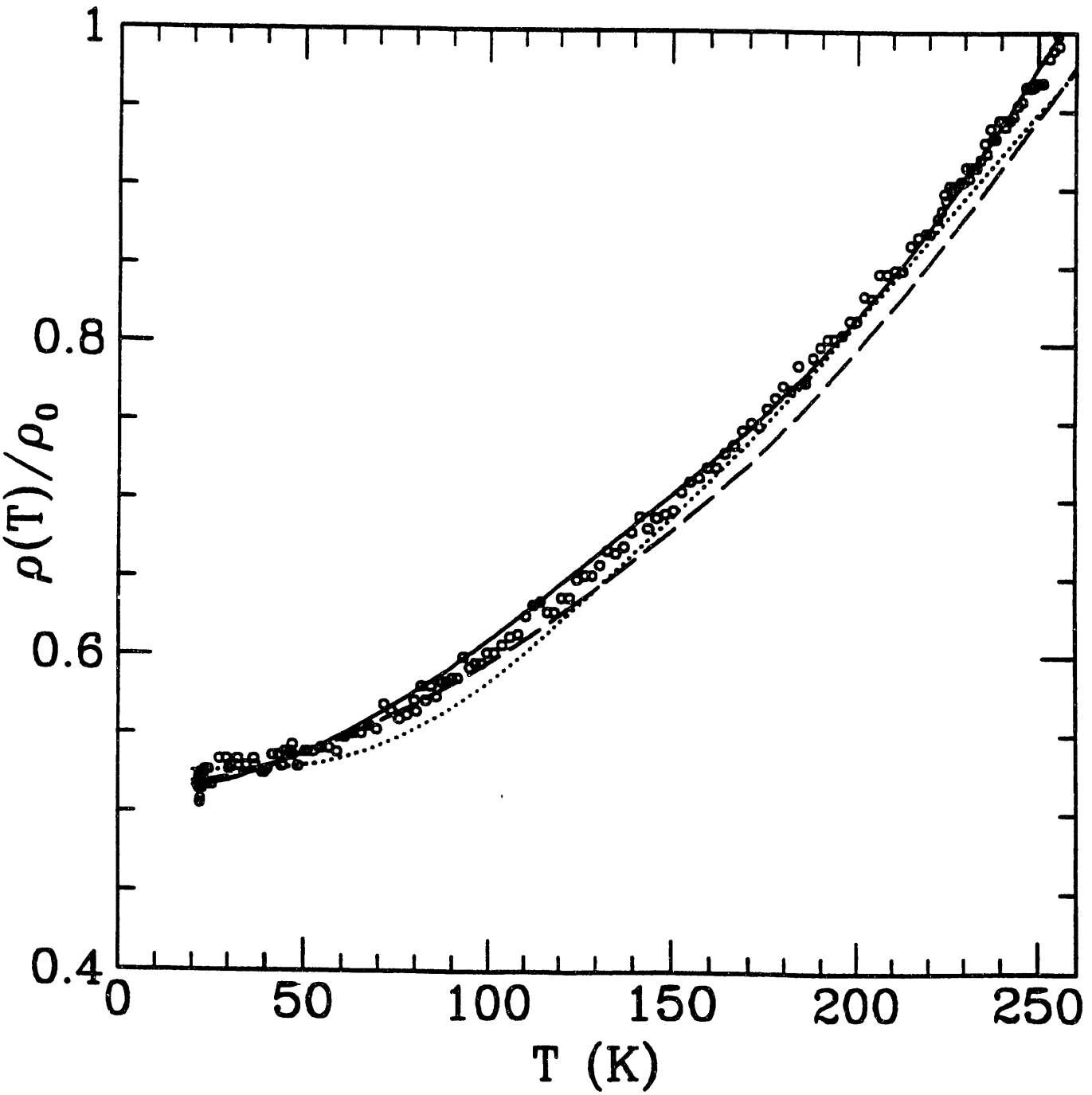

FIG. 2

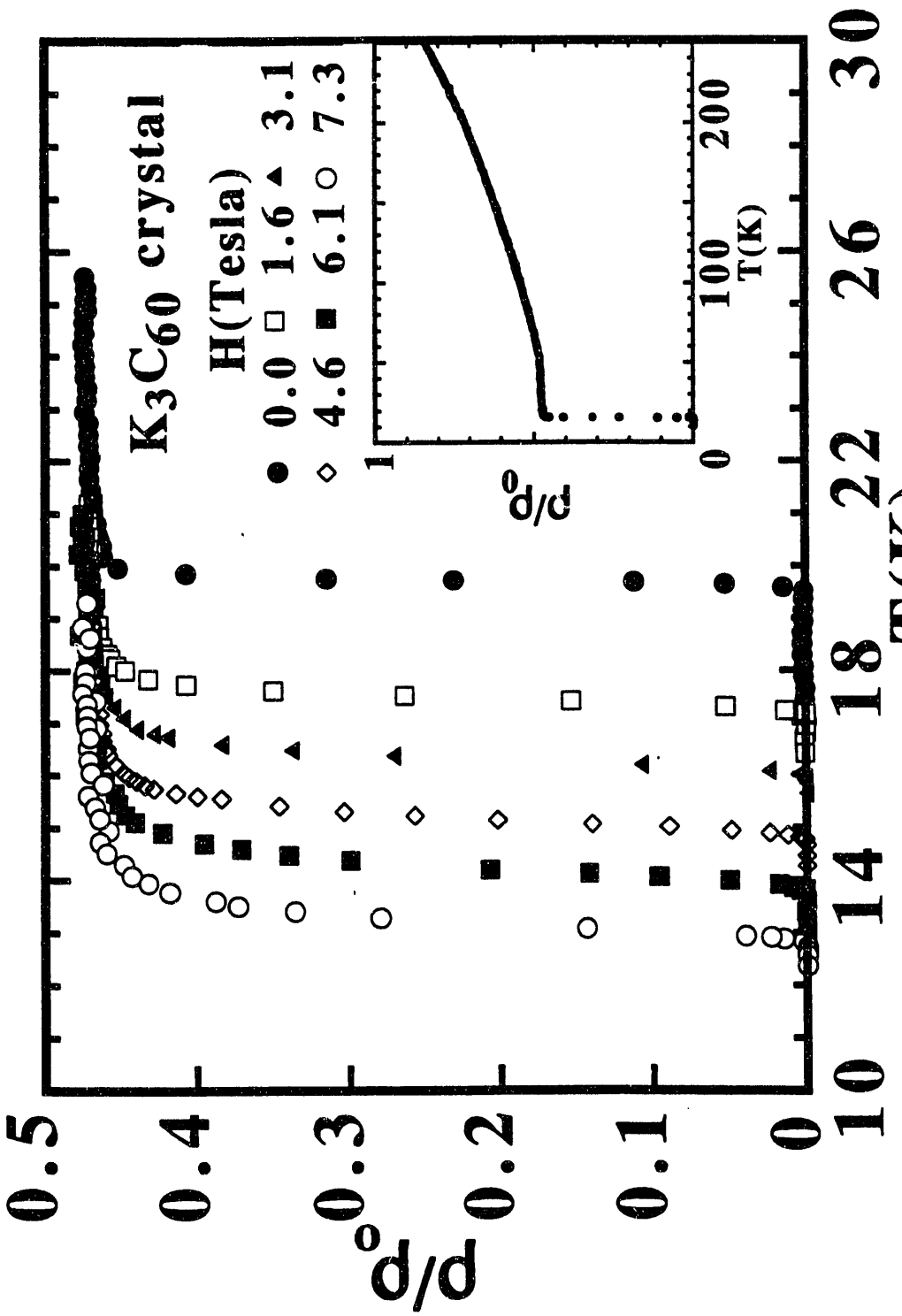
K_3C_{60} crystal
H(Tesla)
0.0
1.6
3.1
4.6
6.1
7.3
ρ/ρ_0
T(K)
0.5
0.4
0.3
0.2
0.1
0
10
14
18
22
26
30
1
0
100
200
T(K)

FIG. 3

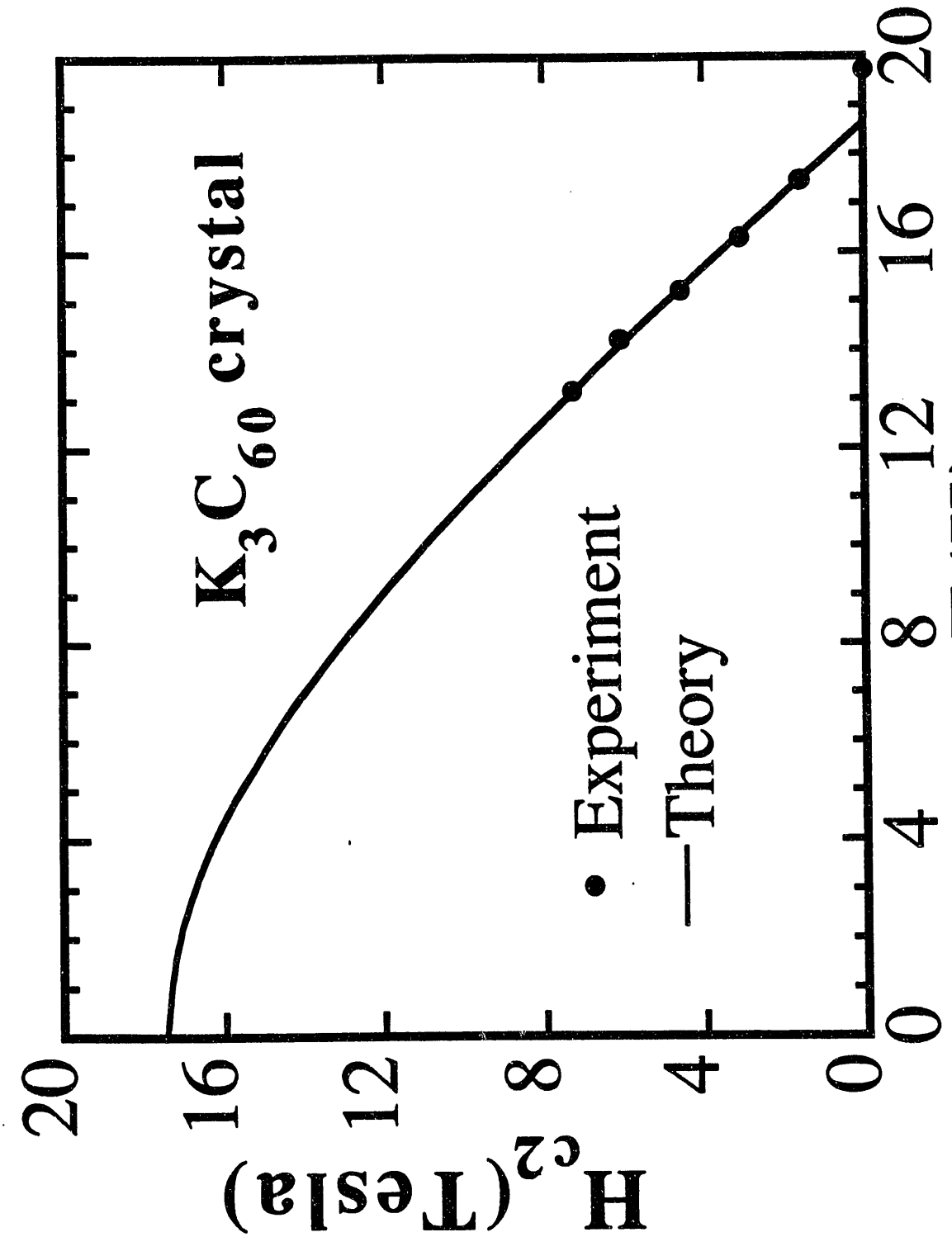

FIG. 4

END

DATE
FILMED
5/03/93